Advancement of photospheric radius expansion and clocked type-I x-ray burst models with the new 22Mg(,p)25 Al reaction rate determined at Gamow energy

Citation for published version:
Hu, J, Yamaguchi, H, Lam, YH, Heger, A, Kahl, D, Jacobs, AM, Johnston, Z, Xu, SW, Zhang, NT, Ma, SB, Ru, LH, Liu, EQ, Liu, T, Hayakawa, S, Yang, L, Shimizu, H, Hamill, CB, Murphy, ASJ, Su, J, Fang, X, Chae, KY, Kwag, MS, Cha, SM, Duy, NN, Uyen, NK, Kim, DH, Pizzone, RG, La Cognata, M, Cherubini, S, Romano, S, Tumino, A, Liang, J, Psaltis, A, Sferrazza, M, Kim, DH, Li, YY & Kubono, S 2021, 'Advancement of photospheric radius expansion and clocked type-I x-ray burst models with the new 22Mg(,p)25 Al reaction rate determined at Gamow energy', *Physical Review Letters*, vol. 127, no. 17, 172701, pp. 1-7. https://doi.org/10.1103/PhysRevLett.127.172701

Digital Object Identifier (DOI):
10.1103/PhysRevLett.127.172701

Link:
Link to publication record in Edinburgh Research Explorer

Document Version:
Peer reviewed version

Published In:
Physical Review Letters

Advancement of photospheric radius expansion and clocked type-I x-ray burst models with the new ^{22}Mg$(\alpha,p)^{25}$Al reaction rate determined at Gamow energy

J. Hu,[1,2,*] H. Yamaguchi,[3,4] Y. H. Lam,[1,2,†] A. Heger,[5,6,7,8] D. Kahl,[9,10] A. M. Jacobs,[8,11] Z. Johnston,[8,11] S. W. Xu,[1] N. T. Zhang,[1] S. B. Ma,[1] L. H. Ru,[1] E. Q. Liu,[1] T. Liu,[1] S. Hayakawa,[3] L. Yang,[3,‡] H. Shimizu,[3] C. B. Hamill,[10] A. St J. Murphy,[10] J. Su,[12] X. Fang,[13] K. Y. Chae,[14] M. S. Kwag,[14] S. M. Cha,[14] N. N. Duy,[14,15] N. K. Uyen,[14] D. H. Kim,[14] R. G. Pizzone,[16] M. La Cognata,[16] S. Cherubini,[16] S. Romano,[16,17,18] A. Tumino,[16,19] J. Liang,[20] A. Psaltis,[20] M. Sferrazza,[21] D. H. Kim,[22] Y. Y. Li,[1,2] and S. Kubono[23]

[1]*Institute of Modern Physics, Chinese Academy of Sciences, Lanzhou 730000, China.*
[2]*School of Nuclear Science and Technology, University of Chinese Academy of Sciences, Beijing 100049, China*
[3]*Center for Nuclear Study(CNS), the University of Tokyo, RIKEN campus, 2-1 Hirosawa, Wako, Saitama 351-0198, Japan*
[4]*National Astronomical Observatory of Japan, 2-21-1 Osawa, Mitaka, Tokyo 181-8588, Japan*
[5]*School of Physics and Astronomy, Monash University, Victoria 3800, Australia*
[6]*OzGrav-Monash – Monash Centre for Astrophysics, School of Physics and Astronomy, Monash University, VIC 3800, Australia*
[7]*Center of Excellence for Astrophysics in Three Dimensions (ASTRO-3D), Australia*
[8]*The Joint Institute for Nuclear Astrophysics, Michigan State University, East Lansing, MI 48824, USA*
[9]*Extreme Light Infrastructure - Nuclear Physics, IFIN-HH, 077125 Bucharest-Măgurele, Romania*
[10]*SUPA, School of Physics & Astronomy, University of Edinburgh, Edinburgh EH9 3FD, United Kingdom*
[11]*Department of Physics and Astronomy, Michigan State University, East Lansing, MI 48824, USA*
[12]*College of Nuclear Science and Technology, Beijing Normal University, Beijing 100875, China*
[13]*Sino-French Institute of Nuclear Engineering and Technology, Sun Yat-Sen University, Zhuhai 519082, Guangdong, China*
[14]*Department of Physics, Sungkyunkwan University, Suwon 16419, Korea*
[15]*Institute of Research and Development, Duy Tan University, Da Nang 550000, Vietnam*
[16]*Laboratori Nazionali del Sud-INFN, Via S. Sofia 62, Catania 95123, Italy*
[17]*Dipartimento di Fisica e Astronomia "Ettore Majorana" - Università degli Studi di Catania*
[18]*Centro Siciliano di Fisica Nucleare e Struttura della Materia (CSFNSM)*
[19]*Facoltà di Ingegneria e Architettura, Università degli Studi di Enna "Kore", Enna 94100, Italy*
[20]*Department of Physics & Astronomy, McMaster University, Ontario L8S 4M1, Canada*
[21]*Département de Physique, Université Libre de Bruxelles, Bruxelles B-1050, Belgium*
[22]*Department of Physics, Ewha Womans University, Seoul 03760, Korea*
[23]*RIKEN Nishina Center, 2-1 Hirosawa, Wako, Saitama 351-0198, Japan*

(Dated: July 22, 2021)

We report the first (in)elastic scattering measurement of ^{25}Al$+p$ with the capability to select and measure in a broad energy range the proton resonances in ^{26}Si contributing to the ^{22}Mg(α,p) reaction at type I x-ray burst energies. We measured spin-parities of four resonances above the α threshold of ^{26}Si that are found to strongly impact the ^{22}Mg(α,p) rate. The new rate advances a state-of-the-art model to remarkably reproduce lightcurves of the GS 1826-24 clocked burster with mean deviation <9% and permits us to discover a strong correlation between the He abundance in the accreting envelope of photospheric radius expansion burster and the dominance of ^{22}Mg(α,p) branch.

Thermonuclear x-ray bursts (XRBs) are the most frequently recorded outbursts that happen in the Galaxy [1–3]. To date, 115 XRB sources have been discovered [4]. More than 62 of the 115 sources categorized as photospheric radius expansion (PRE) bursters [4] of which their bursting mechanism is still an unresolved puzzle due to their intricate hydrodynamics, e.g., the accretion-powered millisecond pulsar SAX J1808.4-3658 [5, 6], which ignited the brightest XRB in recent history [7]. Its first multizone model was recently established [8, 9] and is subject to verification; conversely, it offers a first concurrent sensitivity study on reaction rates for the lightcurves, fluences, and recurrence times, especially the competition between important reactions at a branching point during the onset of an XRB. The GS 1826-24 clocked burster [10–12] is the most investigated due to its nearly consistent accretion rate and lightcurve shape. Its XRB serves as a laboratory to probe the rp-process path [13, 14], compactness [15], and equation of state of the accreting neutron star [16, 17]. Thus, the best model describing the GS 1826-24 lightcurves is highly desired within the community. The first quantitative comparison of its modeled and observed lightcurves could only be achieved 19 years after its discovery [18]; however, up to now, the modeled burst tail does not exactly conform with observation; a similar problem also occurs in

* hujunbaggio@impcas.ac.cn
† lamyihua@impcas.ac.cn
‡ Present address: China Institute of Atomic Energy, P.O. Box 275(10), Beijing 102413, China

other multizone models [15, 19, 20]. It is crucial to verify whether the incapability of the model is due to astrophysical configurations or some influential nuclear reaction rates.

Two recent sensitivity studies performed by Cyburt *et al.* [21] and by Jacobs *et al.* [22] using GS 1826-24 models [18] reveal that the ^{22}Mg(α, p) rate is the most decisive αp-process reaction in *sd*-shell nuclei influencing burst lightcurves, see Supplemental Material (SM) [23]. The ^{22}Mg(α, p) rate proposed by the compilation reaction library REACLIB v2.2 [24], however, is generated using the Hauser-Feshbach (HF) model [25] assuming a rather high level-density of ^{26}Si. This assumption may be invalid and inapplicable considering the selectivity of the (α, p) reaction for natural parity states; moreover, the rate from a high resolution ^{28}Si$(p, t)^{26}$Si measurement [26] was deduced without the experimental information of important resonances within the Gamow window, resulting in a rate up to 6 orders of magnitude lower than the HF-model ^{22}Mg(α, p) rate. Recently, the first direct measurement of the ^{22}Mg(α, p) reaction was performed by Randhawa *et al.* [15]. The evaluated ^{22}Mg(α, p) rate is however based on a rather low ^{22}Mg beam intensity of ∼900 pps which did not permit a direct measurement of ^{22}Mg(α, p) reaction in the Gamow window of XRBs. Only protons with a limited range (90°–120°) were analyzed and the `PACE4` code [27] had to be used to simulate the total cross section. Consequently, they only obtained cross sections corresponding to 2.6 GK. The reaction rates at XRB temperatures (0.7–1.0 GK) were then extrapolated relying on the `TALYS` code, without direct experimental information at the relevant temperature. Such an extrapolation could induce a large additional uncertainty that was not presented in Ref. [15]. Thus, confirming the ^{22}Mg(α, p) rate with precisely measured resonance properties within Gamow window of low uncertainty is crucial to regulate better XRB models to unfold the physics of accreting neutron stars.

In this Letter, we report the first measurement of ^{25}Al + p (in)elastic scattering at x-ray burst energies to deduce the ^{22}Mg$(\alpha, p)^{25}$Al rate. This technique overcomes the difficulties in direct measurement due to the low-cross-section nature of ^{22}Mg(α, p) reaction in the Gamow window. We used the radioactive ion beam separator (CRIB) [28–30] of the University of Tokyo.A primary beam of ^{24}Mg^{8+} at 8.0 MeV/nucleon and 1 eμA bombarded a cryogenic D_2 target [31] to produce a secondary beam of ^{25}Al. The ^{25}Al beam was purified by CRIB using the in-flight method. The ^{25}Al beam, with an energy of 142±1 MeV and an average intensity of 2.0×10^5 pps, was then delivered to the F3 experimental scattering chamber and bombarded a 150-μm-thick CH_2 target, similarly to Ref. [32].

The beam particles were identified event-by-event and the ^{25}Al beam purity was typically 70%. The impurity was mostly ^{24}Mg, clearly discriminated by the timing information.

The recoiling protons were measured using three sets of silicon detector telescopes at central angles of $\theta_{\rm lab}$=0°, 20°, and 23°. Each telescope consisted of a 65-μm-thick and double-sided (16×16 strips) silicon detector and two 1500-μm-thick pad detectors. Protons were clearly identified from other light ions with the $\Delta E{-}E$ method. To identify the inelastic contribution, an array of ten NaI detectors was mounted immediately above the target to detect the γ rays from the decay of excited states of ^{25}Al. Each NaI detector with a geometry of 50×50×100 mm, with the array covering 20% of the total solid angle. These detectors had an average energy resolution of 13.5% in full width at half maximum (FWHM) for 662-keV γ rays. In addition, an 80-μm-thick carbon target was used in a separate run for subtracting the carbon background contribution.

The $E_{c.m.}$ resolution of the excitation function was 30-90 keV (FWHM), depending on the energy, for the Si telescope around $\theta_{\rm lab}$=0°. The uncertainty was mostly from energy straggling of the particles in the thick target, along with the energy resolution of the silicon detectors. At larger angles, the angular resolution of the recoiling proton produced a larger energy uncertainty and the resulting energy resolution was 75-200 keV at $\theta_{\rm lab}$ ∼20°. In this Letter, we focus on the forward angle measurement, where we had the highest resolution to determine the resonance parameters.

The excitation function of ^{25}Al+p elastic scattering has been deduced using the standard procedure as described in Refs. [32–35]. The cross section of inelastic scattering, less than 12% of the elastic scattering, was deduced by analyzing gamma-coincident events as plotted in Fig. 1, and its contribution was subtracted from the total excitation function. The excitation function around $\theta_{\rm lab}$=0° is shown in Fig. 1. Several resonances are clearly evident in the spectrum. To determine the parameters of observed resonances, R-matrix calculations have been performed using `AZURE2` [36] with a channel radius of R=1.4×(1+25$^{1/3}$) fm for the ^{25}Al + p system.

The ground-state spin-parity configurations of ^{25}Al and proton are $5/2^+$ and $1/2^+$, respectively. Thirteen resonances have been analyzed, and the best fit curve is shown in Fig. 1. The resonance properties are listed in Table I. The lowest five states are in good agreement with the previous ^{25}Al + p resonant scattering measurements [37, 38], except the weak 7.379-MeV resonance, where our Γ_{p0} is larger than theirs and the 4^+ assignment by Jung *et al.* [38] cannot reproduce the present data well. The resonances at 8.211 and 8.666 MeV may correspond to the ones observed in Ref. [39], and a spin-parity of 1^- was assigned to the 8.211-MeV resonance based on the mirror assignment. Our analysis shows the assignment as 1^- strongly disagrees with our data, however, whereas 3^+ best matches our data. Bohne *et al.* [40] also discovered the 8.666-MeV state via a ^{24}Mg(^{3}He, n)^{26}Si measurement and a tentative J^π assignment (1^- or 2^+) was made based on a DWBA calculation. Our fitting result disagrees with theirs, but supports the 4^+ assignment made by Matic *et al.* [39]. Although higher resonances had been ob-

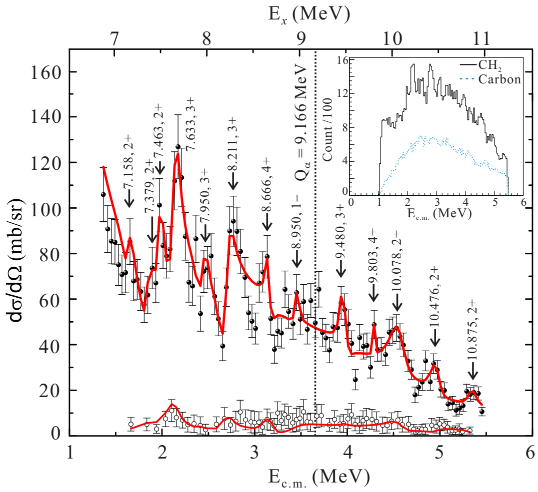

FIG. 1. Excitation function of $^{25}\mathrm{Al} + p$ elastic scattering at $\theta_{\rm lab}$ = 0-8°. Elastic scattering data (filled circles); inelastic scattering data (open circles); the best R-matrix fit (red curve); the α threshold (dotted line); Inset: the $\mathrm{CH_2}$ spectrum with the normalized carbon background.

served by previous studies [26, 41, 42], no J^π was determined. We observed these resonances in the present work, and assigned their tentative J^π with our best R-matrix fit (χ^2/d.o.f.=1.08 for 103 d.o.f). Our presently assigned spin parities generally agree with known states of ^{26}Si. Taking into account all possible assignments for the 9.480-, 9.803-, and 10.078-MeV states, the total $^{22}\mathrm{Mg}(\alpha,p)$ rate changes up to a factor of 0.44 for temperature above 0.7 GK. The minimum χ^2 of the R-Matrix fit supports the 10.476-MeV state to be assigned as 2^+. This state can also be produced via (p,t) reaction [26] which preferentially excites natural-parity states. The 10.875-MeV state can only be either 2^+, 3^+, or 4^+ due to the selection rule of Gamow-Teller transitions [42]. We assign a 2^+ to the 10.875-MeV state, which gives the minimum χ^2. However, the assignments of 3^+ and 4^+ only produce deviations in χ^2 within the standard deviation σ (0.50σ and 0.62σ, respectively), and thus we also consider its possibility as 3^+ or 4^+ in the analysis below as it determines the rate above 1 GK. Further information of the R-matrix analysis is detailed in the SM [23]. To constrain the level properties of the states contributing the reaction rate, we also performed a simultaneous fit for both elastic and inelastic scattering data. With the limit of inelastic scattering data, we obtained the upper limits of inelastic proton widths, $\Gamma_{p1,\max}$ (Table II).

The ^{26}Si levels above the α threshold are expected to characterize the $^{22}\mathrm{Mg}(\alpha,p)$ rates. As the widths are broad for the 10.078-, 10.476-, and 10.875-MeV states, we applied the broad-resonance approximation, in which the reaction rates can be obtained from [43],

$$N_A\langle\sigma v\rangle = \sqrt{2\pi}\frac{N_A\hbar^2}{(\mu kT)^{3/2}}\sum_i \omega_i \int_0^\infty e^{-E/kT} \times \frac{\Gamma_\alpha(E)\Gamma_p(E+Q)}{(E-E_R^i)^2+\Gamma(E)^2/4} dE\,[\mathrm{cm^3s^{-1}mol^{-1}}]\,. \quad (1)$$

Here, μ is the reduced mass of the target and projectile, T is the temperature, E_R is the energy of the resonance, and the statistical factor ω=$2J_i+1$. The energy dependence of the widths was taken into account by letting the partial widths Γ_α and Γ_p vary as, $\Gamma_x^i(E) = \Gamma_x^i(E_R^i)\frac{P_\ell(E)}{P_\ell(E_R^i)}$ where the P_ℓ are the Coulomb penetrabilities for the α and p channels, respectively. The partial width $\Gamma_p(E_R)$ is from our R-matrix fit, and $\Gamma_\alpha(E_R)$ can be inferred from the mirror nucleus ^{26}Mg via the isospin symmetry relation, Γ_α^i=$C^2S_\alpha\Gamma_\alpha^{i,\mathrm{SP}}$, where the C^2S_α is the α-spectroscopic factor and $\Gamma_\alpha^{\mathrm{SP}}$ is the single-particle α width. We adopted the average C^2S_α values from Ref. [26]; $C^2S_\alpha(4^+)$=0.015 and $C^2S_\alpha(2^+)$=0.037, with uncertainties of a factor of 2, as in [44]. Table II shows the adopted resonance parameters in obtaining the $^{22}\mathrm{Mg}(\alpha,p)$ rates, which are shown together with the rates from the HF model (hereinafter NON-SMOKER) [25] and Matic *et al.* [26] in Fig. 2. The resonance J^π(10.875 MeV)=3^+ does not contribute to the $^{22}\mathrm{Mg}(\alpha,p)$ rate whereas the contribution from assuming it as 4^+ is much lower than assuming it as 2^+. Both possible $^{22}\mathrm{Mg}(\alpha,p)$ rates assuming J^π(10.875 MeV)=3^+ or 4^+ are similar and the difference in reaction rate is only up to a factor of 0.27. Note that in the critical temperature range for XRB ignition, the NON-SMOKER $^{22}\mathrm{Mg}(\alpha,p)$ rate differs from ours by a factor of ~10 from ~0.4 to ~1 GK, and varies up to a factor of ~160 at 3 GK. Due to the missing resonance data of ^{26}Si above 10 MeV excitation energy in Matic *et al.* [26], there is a discrepancy of about 1 to 5 orders of magnitude between our new rate and the Matic *et al.* rate for T=0.7–3 GK (Fig. 2). The $^{22}\mathrm{Mg}(\alpha,p)$ rate by Randhawa *et al.* [15] approximated with the NON-SMOKER $^{22}\mathrm{Mg}(\alpha,p)$ rate divided by 8, is also shown in Fig. 2. Although their evaluated rate does not largely deviate from our present rate at around 1 GK and below, we caution that their evaluation may underestimate the uncertainty due to the theoretical extrapolation without considering each resonance explicitly. Our $^{22}\mathrm{Mg}(\alpha,p)$ rate has a significantly lower uncertainty than theirs (Fig. 2) even if such possible underestimation is ignored, see SM [23] for the further error estimation. Our final rate is merely enhanced by at most 10% when considering the additional $\Gamma_{p1,\max}$.

GS 1826-24 clocked burster: To quantitatively compare with the GS 1826-24 burster (Fig. 3), we adopt the best fit model from Jacobs *et al.* [22], which has a ratio of accreted ^{1}H to ^{4}He of 2.39, a CNO metal mass fraction of 0.0075, and an accretion rate of $3.325\times10^{-9}\ M_\odot\mathrm{yr}^{-1}$, as our *baseline* model. We update it with the present $^{22}\mathrm{Mg}(\alpha,p)$ rate to represent the *Present* model. The generated burst luminosity, L_x, by the 1D multizone hydrodynamic KEPLER code [18, 47] is related to observational flux, F_x by scaling with $\left[4\pi d^2\xi_b(1+z)^2\right]^{-1}$ [48], where d is the distance, ξ_b incorporates the possible burst-emission anisotropy, and the redshift, z, expands the lightcurve when transforming into an observer's frame. Instead of specifically selecting data close to the burst peak at t=−10 to 40 s [15, 20], we impartially select all observational data of the entire burst timespan to

TABLE I. The presently determined energy levels of ^{26}Si compared with literature.

	^{26}Si present work			^{26}Si from other works			
No.	E_x (MeV)[a]	J^π	Γ_{p0}[b] (keV)	E_x (MeV)	J^π	Γ_{p0} (keV)	Refs.
1.	7.158(13)	2^+	6(3)	7.162(14) / 7.147(27)	2^+	7(4) / 2.7(1)	[37] / [38]
2.	7.379(18)	2^+	28(14)	7.402(40) / 7.401(28)	2^+ / 4^+	6(4) / 1.1(1)	[37] / [38]
3.	7.463(18)	2^+	51(9)	7.484(13) / 7.484(28)	2^+	46(11) / 15.9(3)	[37] / [38]
4.	7.633(20)	3^+	46(8)	7.704(13) / 7.654(29)	3^+ / (2^+, 3^+)	41(6) / (30.1(5), 19.5(3))	[37] / [38]
5.	7.950(22)	3^+	10(5)	8.015(14) / 7.977(30)	3^+ / (2^+, 3^+)	15(5) / (4.5(3), 3.6(2))	[37] / [38]
6.	8.211(24)	3^+	48(10)	8.222(5)	1^-		[39]
7.	8.666(25)	4^+	8(5)	8.700(30) / 8.687(12)	(1^-, 2^+) / (4^+)		[39] / [40]
8.	8.950(30)	1^-	16(5)	8.952(7)			[41]
9.	9.480(30)	3^+	15(4)	9.433(4)			[42]
10.	9.803(32)	4^+	2(1)	9.802(7)			[41]
11.	10.078(36)[c]	2^+	164(30)	10.070(8)			[41]
12.	10.476(40)	2^+	54(22)	10.436(10)			[26]
13.	10.875(45)	2^+	57(21)	10.827(8)			[42]

[a] Statistical errors due to the R-matrix fit folded with systematic uncertainty of 12-35 keV is given in parentheses.
[b] Elastic scattering proton widths.
[c] An 1^+ assignment is not excluded, but not preferred from the inelastic data and its influence on the final reaction rate is negligible.

TABLE II. Resonance parameters for the ^{22}Mg(α,p) rates.

E_x (MeV)	J^π	Γ_α (eV)	Γ_{p0} (keV)	$\Gamma_{p1,max}$ (keV)
9.803(32)	4^+	9.69×10^{-13}	2(1)	5.9×10^{-3}
10.078(36)	2^+	1.13×10^{-6}	164(30)	22.6
10.476(40)	2^+	1.80×10^{-3}	54(22)	9.9
10.875(45)	2^+	1.70×10^{-1}	57(21)	1.0

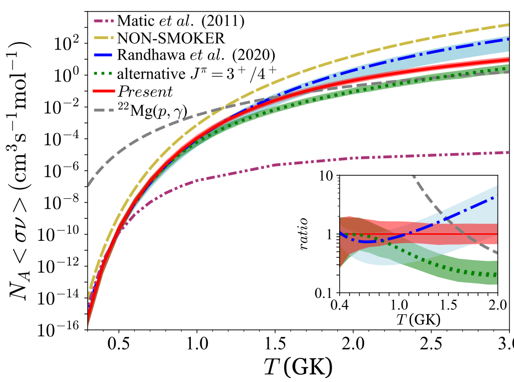

FIG. 2. The ^{22}Mg(α,p) rates. The uncertainty of the present rate (red zone) is estimated via Monte-Carlo calculation [45] considering all errors from the present experimental measurement. Both possible rates with J^π(10.875 MeV)=3^+ or 4^+ are not distinguishable, plotted as a green line and labeled as "alternative J^π=$3^+/4^+$". Randhawa *et al.* [15] rate uncertainty is the blue zone. Inset: the ratios of Randhawa *et al.*, or "alternative J^π=$3^+/4^+$" or ^{22}Mg(p,γ) [24, 46] rate to the present ^{22}Mg(α,p) rate.

fit our modeled bursts. The modeled bursts are averaged and fitted to the averaged lightcurve of GS 1826-24 epoch *Jun 1998* [49], which were recorded by the *Rossi X-ray Timing Explorer* (RXTE) Proportional Counter Array [4, 50, 51].

The *baseline* lightcurve at t=16–76 s is enhanced and the discrepancy with observed data becomes only up to 6% due to the present and lower ^{22}Mg(α,p) rate, which at low temperature competes with ^{22}Mg$(\beta\nu)$ decay and overcomes ^{22}Mg(p,γ) at higher temperature T>$1.67^{+0.15}_{-0.13}$ GK instead of at T>1.16 GK compared to the NON-SMOKER ^{22}Mg(α,p) rate (Fig. 2). The alternative J^π=$3^+/4^+$ rate yields only 3% deviation from the observed data at t=16–76 s, which is not discernible in Fig. 3. The matter flow is more siphoned out to ^{22}Mg$(p,\gamma)^{23}$Al$(p,\gamma)^{24}$Si(α,p), enriching more proton-rich nuclei nearer to dripline past the *sd*-shell. These nuclei burn hydrogen after the burst peak and enhance the lightcurve at t=16–76 s, depleting hydrogen that is to be burnt by further (p,γ) reactions at later time t=80–150 s. Hence, the observed lightcurve profile at t=80–150 s is noticeably reproduced. Therefore, the present work experimentally validates the predicted lightcurve trend in Ref. [21] and enhances a state-of-the-art model to remarkably reproduce the GS 1826-24 lightcurve with mean deviation <9 %, see SM [23]. In the latest model by Randhawa *et al.* [15] (the blue line in Fig. 3), a similar trend is manifested at t=8–64 s, however, it deviates their baseline model farther away from observation and affects their fitted redshift-distance.

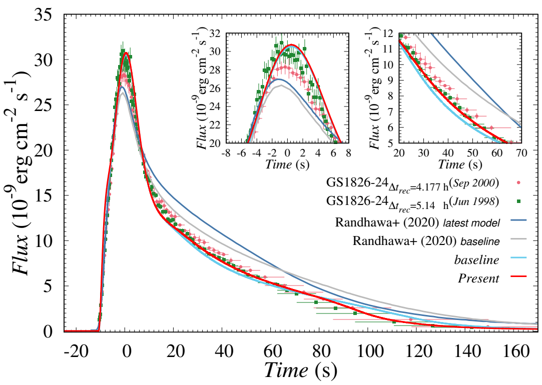

FIG. 3. The best fit *baseline* and *Present* modeled lightcurves to the observed lightcurve of epoch *Jun 1998*, and the best fit Randhawa *et al.* [15] lightcurves to epoch *Sep 2000*. The magnified lightcurves at the burst peak and t=20–70 s are shown in the left and right insets, respectively.

SAX J1808.4-3658 PRE burster: The initial good-fit SAX J1808.4-3658 PRE models constructed by Johnston *et al.* [8] and studied by Goodwin *et al.* [9] are based on the KEPLER code using the NON-SMOKER ^{22}Mg(α,p) rate

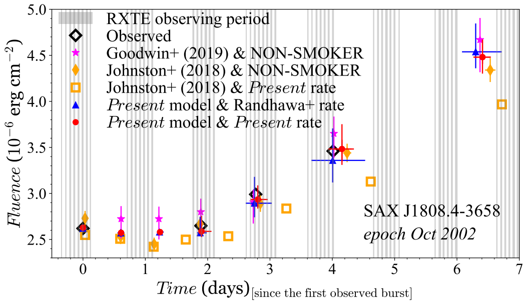

FIG. 4. The bursts' fluences (integration of flux over time) and times for SAX J1808.4-3658 burster, based on the RXTE observation [4], Johnston *et al.* [8] and Goodwin *et al.* [9] models, and present calculations. Johnston *et al.* [8] model is adopted to study the present and Randhawa *et al.* rates.

but these models can still provide us a unique and sensitive study for competition between the ^{22}Mg(α,p) and ^{22}Mg(p,γ) reactions because the temperature of competition between both reactions, T_C (the intersection of ^{22}Mg(α,p) and ^{22}Mg(p,γ) [24, 46] rates in inset of Fig. 2), is within the range of accreting-envelope maximum temperature, $1.1\leqslant T_{\rm max}/{\rm GK}\leqslant 1.6$, during a typical PRE burst, and the He and H abundances are almost equal in the accreting envelope of SAX J1808.4-3658 PRE burster [8, 9]. The present ^{22}Mg(α,p) rate which has the lowest uncertainty among all available rates precisely locates the T_C=$1.67^{+0.15}_{-0.13}$ GK constricting the ^{22}Mg(α,p) branch. With our new rate, the previous model parameters do no longer well reproduce the observation (orange squares in Fig. 4). With only constraining the He abundance in the accreting envelope to be $X_{\rm He}$=56.7±0.3%, we successfully regulated the ^{22}Mg(α,p) and ^{22}Mg(p,γ) branches and improved the modeled fluences closer to observation (red dots in Fig. 4). The He-abundance constraint reveals a strong correlation with the dominance of ^{22}Mg(α,p) branch and introduces a striking advancement for the pioneering PRE model. The approximated ^{22}Mg(α,p) rate [15] with large uncertainty, however, estimates a wide range of T_C=1.4–1.8 GK; also the propagation of their rate uncertainty yields a less constrained range of He abundance $X_{\rm He}$=56.1±1.1 causing large uncertainty in fluences and times (blue triangles in Fig. 4).

In summary, we have performed the first (in)elastic scattering measurement of $^{25}{\rm Al}+p$ with the capability to select and measure proton resonances contributing to the ^{22}Mg$(\alpha,p)^{25}$Al reaction at XRB temperature. This provides the spectroscopic information of four resonances above the α threshold of ^{26}Si that strongly influence the ^{22}Mg$(\alpha,p)^{25}$Al reaction rate. We successfully deduced the ^{22}Mg$(\alpha,p)^{25}$Al rate via experiment without implementing a scaling factor on a Hauser-Feshbach statistical model rate as was done in Ref. [15]. The improved nuclear physics input permits us to better reproduce the observed GS 1826-24 lightcurves than the previous model (see SM [23]) and to further constrain the SAX J1808.4-3658 model.

This experiment was performed at the RI Beam Factory operated by RIKEN Nishina Center and CNS, University of Tokyo. We would like to thank the CRIB and RIKEN accelerator staffs for their dedication to this project. We thank D. Galloway for stimulating discussions and help in the comparison with GS 1826-24 and SAX J1808.4-3658 XRB sources. This work is financially supported by the Major State Basic Research Development Program of China (2016YFA0400503, 2016YFA0400501, and 2016YFA0400504), the Strategic Priority Research Program of Chinese Academy of Sciences, Grant No. XDB34020204, JSPS KAKENHI (Nos. 16K05369, and 19K03883), the Ministry of Education, Culture, Sports, Science and Technology (MEXT) of Japan, Chinese Academy of Sciences President's International Fellowship Initiative (No. 2019FYM0002). Y.H.L. and K.Y.C. thank the National Natural Science Foundation of China (Nos. 11775277, 31211775277). The Edinburgh group is appreciative of funding from the UK STFC. A.H. is supported by the Australian Research Council Centre of Excellence for Gravitational Wave Discovery (OzGrav, No. CE170100004) and for All Sky Astrophysics in 3 Dimensions (ASTRO 3D, No. CE170100013). K.Y.C. was supported by National Research Foundation of Korea (Nos. 2020R1A2C1005981, 2019K2A9A2A10018827, and 2016R1A5A1013277). M.S. is supported from Fonds de la Recherche Scientifique - FNRS Grant Number 4.45.10.08. Y.H.L. and A.H. deeply appreciate the computing resources provided by the Institute of Physics (PHYS_T3 cluster) and the ASGC (Academia Sinica Grid-computing Center) Distributed Cloud resources (QDR4 cluster) of Academia Sinica, Taiwan, and Gansu Advanced Computing Center.

[1] W. H. G. Lewin *et al.*, Space Sci. Rev. **62**, 223 (1993).
[2] H. Schatz *et al.*, Nucl. Phys. **A 777**, 601 (2006).
[3] A. Parikh *et al.*, Prog. Part. Nucl. Phys. **69**, 225 (2013).
[4] D. K. Galloway *et al.*, Astrophys. J. Suppl. **249**, 32 (2020).
[5] R. Wijnands and M. van der Klis, Nature **394**, 344 (1998).
[6] D. Chakrabarty *et al.*, Nature **424**, 42 (2003).
[7] P. Bult *et al.*, Astrophys. J. Lett. **885**, L1 (2019).
[8] Z. Johnston *et al.*, Mon. Not. R. Astron. Soc. **477**, 2112 (2018).
[9] A. Goodwin *et al.*, Mon. Not. R. Astron. Soc. **490**, 2228 (2019).
[10] F. Makino *et al.*, IAU Circ. , No. 4653 (1988).
[11] Y. Tanaka, in *Proc. 23rd ESLAB Symp., Two Topics in X-Ray Astronomy*, edited by J. Hunt and B. Battrick (SP-296; Noordwijk: ESA, 1989) p. 3.
[12] P. Ubertini *et al.*, Astrophys. J. Lett. **514**, L27 (1999).

[13] H. Schatz *et al.*, Phys. Rep. **294**, 167 (1998).
[14] J. L. Fisker *et al.*, Astrophys. J. Suppl. **174**, 261 (2008).
[15] J. S. Randhawa *et al.*, Phys. Rev. Lett. **125**, 202701 (2020).
[16] A. W. Steiner *et al.*, Astrophys. J. **722**, 33 (2010).
[17] A. Dohi *et al.*, Prog. Theor. Exp. Phys. **2020**, 033E02 (2020).
[18] A. Heger *et al.*, Astrophys. J. Lett. **671**, L141 (2007).
[19] B. Paxton *et al.*, Astrophys. J. Suppl. **220**, 15 (2015).
[20] Z. Meisel, Astrophys. J. **860**, 147 (2018).
[21] R. Cyburt *et al.*, Astrophys. J. **830**, 55 (2016).
[22] A. M. Jacobs, A. Heger, Z. Johnston, *et al.*, Multi-zone x-ray burst reaction rate sensitivities, in *Talk at Burst Environment, Reactions and Numerical Modelling Workshop, Monash Prato Centre, Tuscany, Italy* (2018).
[23] See Supplemental Material at [URL] for all the possible spin-parity tests of the dominant resonant states 10.078-MeV, 10.476-MeV, and 10.875-MeV; further estimation of the *Present* ^{22}Mg(α,p)^{25}Al reaction rate uncertainty; the evidence indicating the importance of ^{22}Mg(α,p)^{25}Al reaction.
[24] R. Cyburt *et al.*, Astrophys. J. Suppl. **189**, 240 (2010).
[25] `http://nucastro.org/nonsmoker.html`.
[26] A. Matic *et al.*, Phys. Rev. **C 84**, 025801 (2011).
[27] O. Tarasov and D. Bazin, Nucl. Instr. Meth. **B 266**, 4657 (2008).
[28] Y. Yanagisawa *et al.*, Nucl. Instr. Meth. **A 539**, 74 (2005).
[29] S. Kubono *et al.*, Eur. Phys. J. **A 13**, 217 (2002).
[30] H. Yamaguchi *et al.*, Nucl. Phys. News **30**, 21 (2020).
[31] H. Yamaguchi *et al.*, Nucl. Instr. Meth. **A 589**, 150 (2008).
[32] H. Yamaguchi *et al.*, Phys. Lett. **B 672**, 230 (2009).
[33] T. Teranishi *et al.*, Phys. Lett. **B 556**, 27 (2003).
[34] T. Teranishi *et al.*, Phys. Lett. **B 650**, 129 (2007).
[35] J. J. He *et al.*, Phys. Rev. **C 76**, 055802 (2007).
[36] R. E. Azuma *et al.*, Phys. Rev. **C 81**, 045805 (2010).
[37] J. Chen *et al.*, Phys. Rev. **C 85**, 015805 (2012).
[38] H. S. Jung *et al.*, Phys. Rev. **C 90**, 035805 (2014).
[39] A. Matic *et al.*, Phys. Rev. **C 82**, 025807 (2010).
[40] W. Bohne *et al.*, Nucl. Phys. **A 378**, 525 (1982).
[41] Y. Shimizu *et al.*, in *Proc. of the Int. Symposium on the Origin of Matter and Evolution of Galaxies* (World Scientific, Singapore, 2005) p. 367.
[42] J. C. Thomas *et al.*, Eur. Phys. J. **A 21**, 419 (2004).
[43] C. Iliadis, *Nuclear Physics of Stars* (Wiley, Weinheim, 2007).
[44] C. D. Nesaraja *et al.*, Phys. Rev. **C 75**, 055809 (2007).
[45] W. J. Thompson *et al.*, Nucl. Phys. **A 647**, 259 (1999).
[46] C. Iliadis *et al.*, Nucl. Phys. **A 841**, 31 (2010).
[47] S. Woosley *et al.*, Astrophys. J. Suppl. **151**, 75 (2004).
[48] Z. Johnston *et al.*, Mon. Not. R. Astron. Soc. **494**, 4576 (2020).
[49] D. K. Galloway *et al.*, Pub. Astron. Soc. Aust. **34**, e019 (2017).
[50] D. K. Galloway *et al.*, Astrophys. J. **601**, 466 (2004).
[51] D. K. Galloway *et al.*, Astrophys. J. Suppl. **179**, 360 (2008).